Variable Frequency Controlled Two-Load Induction Cooking System

R Snehalatha
Department of Electrical Engineering
National Institute of Technology Warangal, India

N Vishwanathan
Department of Electrical Engineering
National Institute of Technology Warangal, India

S Porpandiselvi
Department of Electrical Engineering
National Institute of Technology Warangal, India. **Email:** selvi@nitw.ac.in

Abstract- two-load induction heating system is presented using variable frequency control. Both loads are operated with different frequencies. A H-bridge inverter output powers both loads. Series resonant concept is used with each load circuit. Each leg of the bridge inverter operates at different frequency. Load power control is achieved by variation of the operating frequency of each leg. Simulation results validate the performance of the presented system. High efficiency is possible due to soft switching operation of the inverter.
Keywords – Series resonant inverter, IH cooking, variable frequency control

I. INTRODUCTION

Cooking by means of electrical power is gaining importance in the form of Induction heating. Various benefits of induction cooking are like cleanliness, safety, accurate, good efficiency, fast control etc. Generally large frequency alternating current circulates through the heating coil inducing emf in the vessel mounted on it. In turn it heats the vessel. Depth of penetration of currents is expressed by the following expression.

$$\delta = \sqrt{\frac{\rho}{\pi \mu f_s}}$$

Where ρ is the resistivity and μ is the magnetic permeability of the vessel. fs is the operating frequency of the source. Usually, the coil has high inductance which results in low power factor. To compensate this a capacitor is connected in series which resonates with inductance forming series resonant circuit.

Induction coil is like the primary of the transformer and the vessel is like a single turn secondary coil of the transformer. The resistance of the vessel when reflected to the coil form a series R L C resonant circuit. Generally the resonant frequency is 10% lower than the operating frequency for zero voltage switching (ZVS) operation of the inverter. This results in higher efficiency. There are several control techniques available in the literature for the control of inverter. Half bridge or full bridge resonant converter can be used for producing high frequency voltage [1]-[4]. The control techniques used are Pulse amplitude modulation (PAM), Pulse frequency modulation (PFM). In PAM source voltage can be controlled for output power control. In PFM variable frequency operation can be used which varies the admittance of the load circuit and controls the power transferred. Other control techniques like Power density modulation (PDM) [5]-[6] Phase shift control (PSC), Asymmetric duty cycle control (ADC), Asymmetric voltage cancellation control (AVC) are also popular [7]. [8] Proposes a hybrid power control technique combining pulse density and PSM technique.

Presently, there is a trend for the development of multiple-load induction cooking system. In this type of applications, more number of heating coils are present. They need to be powered such that independent control of each load is possible. The design requirements are such that the component count of the power inverter should be less and independent control should be possible without much complexity. Certain configurations are available in the literature. [9] Proposes a 3-leg inverter powering two loads with independent control. In this configuration AVC technique is employed. Another configuration with two-loads and single inverter is proposed in [10]. In this configuration variable frequency control is used. [11-13] also give some more methodologies for induction heating applications.

This paper proposes a two-load induction cooking system with independent control. A H-bridge inverter power these loads. Each leg of the inverter is operated at different switching frequency. Both loads have resonant frequencies which are slightly less than the switching frequencies. By control of each leg frequency, the impedance of the corresponding load is controlled and then power is controlled. This configuration offers less component count, independent control of loads and significant efficiency.

II. PROPOSED SYSTEM

H-bridge inverter circuit is shown in Fig:1. In this application two loads are used. In this full-bridge resonant inverter where Q_1, Q_2, Q_3 and Q_4 are the MOSFET switches and D_1, D_2, D_3 and D_4 are body diodes of the MOSFETs. A dc voltage of V_{DC} is supplied to the full-bridge inverter. The induction heating (IH) load is represented as series R-L-C circuit. C is added in series to IH load for improvement of power factor. Both loads are connected at the output terminals of H-bridge inverter i.e, X and Y. First load (L_1) is composed of L_{r1}, R_{eq1} and C_{r1}. Similarly, load-2 consists of L_{r2}, $R_{eq2}$and C_{r2}.

978-1-5386-6159-8/18/$31.00 © 2018 IEEE

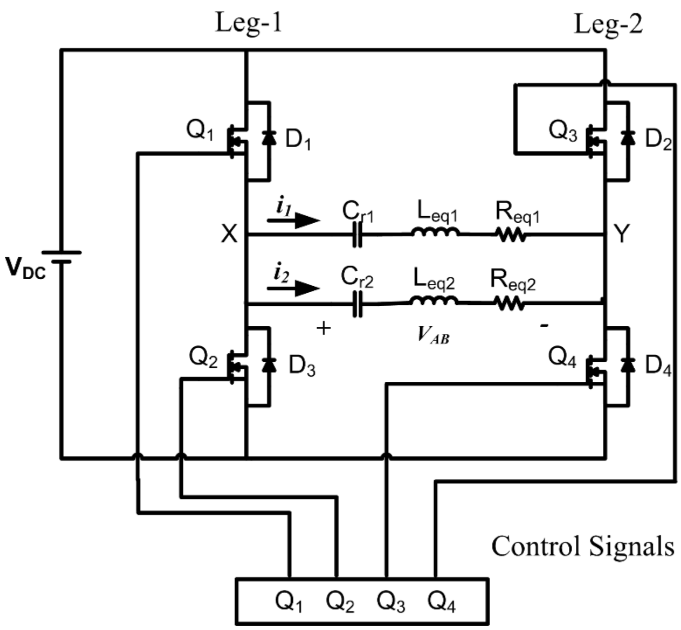

Fig. 1 Proposed inverter configuration

III. PRINCIPLE OF OPERATION

In the proposed system, leg-1 is switched at low frequency and leg-2 is switched at high frequency. L_1 is tuned for low frequency and L_2 is tunes for high frequency. L_1 conducts mainly low frequency current and L_2 conducts mainly high frequency current. Thereby, independent control of the two resonant circuits i.e., the two loads is possible. Both legs are operated with fixed 50% duty cycle. Here variable frequency control is employed where, each leg frequency is controlled independently to control the corresponding resonant circuit output power.

Both loads are connected across the same output terminals, for independent control, each leg is operated with different switching frequency. Low and high switching frequencies of L_1 and L_2 should be selected such that one frequency components should not affect the other load components. Wide operating frequency range (20-200 kHz) is used in IH application. Therefore, in the proposed full-bridge inverter topology, inverter leg-1 is operated with low frequency, f_1 = 30 kHz, and inverter leg-2 is operated with high frequency, f_2 = 200 kHz.

Resonant frequencies of L_1 and L_2 are $f_{r1}=\frac{1}{2\pi\sqrt{L_{eq1}C_{r1}}}$ and $f_{r2}=\frac{1}{2\pi\sqrt{L_{eq2}C_{r2}}}$. Generally f_{r1} and f_{r2} are chosen 10% below the operating frequencies. Various parameters of the H-bridge inverter and loads are mentioned in Table A. Here, $L_{eq1} = L_{eq2}$ and $C_{r1} > C_{r2}$ and $f_{s1} < f_{s2}$.

Fig:2 presents equivalent circuits for L_1 and L_2. When inverter is operated at f_{s1}, X_{cr2} is very high such that C_2 acts as open circuits. Therefore, the low frequency current mainly flows through R_{eq1}, L_{r1} and C_{r1}. The impedance of first load (L_1) is

$$Z_{eq1} = R_{eq1} + \left(j2\pi f_{s1}L_{r1} - j\frac{1}{2\pi f_{s1}C_{r1}}\right)$$

When the inverter is operated at f_{s2}, X_{Leq1} is very high such that L_1 acts as open circuit. Hence, the high frequency current mainly flows through R_{eq2}, L_{eq2} and C_{r2}. The impedance of second load (L_2) is,

$$Z_{eq2} = R_{eq2} + \left(j2\pi f_{s2}L_{eq2} - j\frac{1}{2\pi f_{s2}C_{r2}}\right)$$

Load characteristics of L_1 and L_2 are shown in Fig:3. They also indicate that impedance is minimum at resonant frequencies with zero phase angle.

TABLE A H-bridge and load parameters

Parameter	Value
Supply voltage, V_{dc}	48 V
Reflected resistance of L_1, R_{eq1}	1.95 Ω
Reflected inductance of L_1, L_{eq1}	68 uH
Reflected resistance of L_2, R_{eq2}	2.6 Ω
Reflected inductance of L_2, L_{eq2}	68 uH
Resonant capacitor of load-1, C_{r1}	0.45 uF
Resonant capacitor of load-2, C_{r2}	0.01 uF
Switching frequency, f_{s1}	30 kHz
Switching frequency, f_{s2}	200 kHz

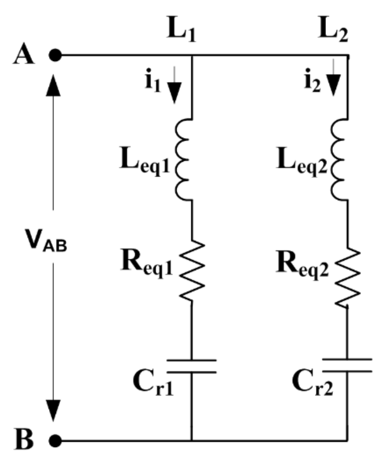

Fig. 2 load circuits of L_1 and L_2

IV. OUTPUT POWER CONTROL

Gate signals of H-bridge inverter v_{g1}, v_{g2}, v_{g3} and v_{g4} are shown in Fig. 4. v_{g1} and v_{g2} are applied to leg-1 of the inverter operated with low frequency switching pulses and 50% duty cycle. v_{g3} and v_{g4} are applied to leg-2 of the inverter operated with high frequency switching pulses and 50% duty cycle. Both legs are operated with fixed 50% duty cycle.

Here variable frequency control is employed where, each leg switching frequency is controlled independently to control the corresponding resonant circuit output power. Low frequency is varied from 30 kHz to 50 kHz and high frequency is varied from 200 kHz to 230 kHz for individual load power control.

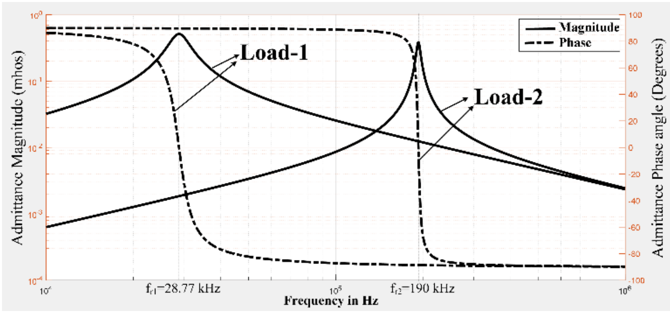

Fig. 3 Admittance characteristics of the loads

Total output power is the sum of powers of L_1 and L_2.
Load power of L_1 is

$$P_{o1} = I_{o1}^2 \; R_{eq1}$$

where, I_{o1} is the effective current in L_1.
Load power of L_2 is

$$P_{o2} = I_{o2}^2 \; R_{eq2}$$

where, I_{o2} is the effective current in L_2.

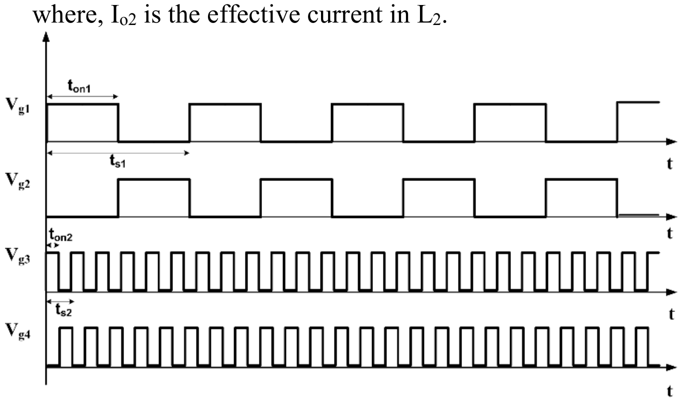

Fig. 4 Gate signals of H-bridge inverter

V. Simulation Results

IH load system presented in this paper is simulated and the waveforms are presented in Figs. 5-14. Fig. 5 displays the simulated result of inverter voltage, v_{XY}, current in L_1 , i_{L1} and current in L_2, i_{L2} for normal switching frequencies of f_{s1} = 30 kHz and f_{s2} = 200 kHz. Fig. 6 shows the Fourier analysis of both load currents for normal switching frequencies which shows that currents in L_1 and L_2 are mainly desired frequency currents of those particular loads. Other harmonic currents are absent in each load. Hence operation of one load is not affected by the other.

Fig. 9-10 shows the independent control of load-2 by varying leg-2 higher switching frequency and keeping the leg-1 lower switching frequency fixed. Fig.7 shows v_{AB}, i_{L1} and i_{L2} waveforms at f_{s1} = 30 kHz and f_{s2} = 210 kHz. Fig. 8 shows corresponding load current Fourier analysis at the above switching frequencies. Similarly, Fig. 9 shows v_{AB}, i_{L1} and i_{L2} waveforms at f_{s1} = 30 kHz and f_{s2} = 220 kHz and Fig. 10 shows corresponding load current Fourier analysis at the above switching frequencies.

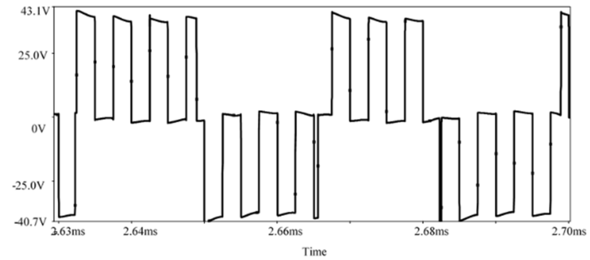

(a)

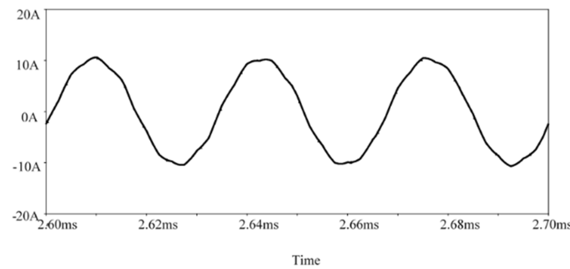

(b)

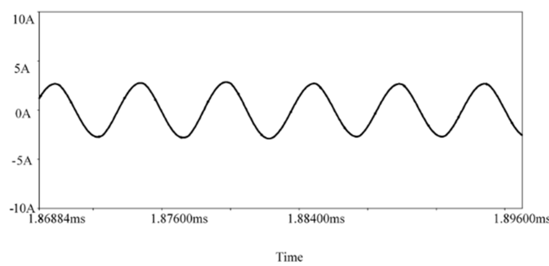

(c)

Fig. 5 Simulation waveforms with f_L = 30 kHz, f_H = 200 kHz
(a) v_{AB} of the proposed configuration
(b) i_{L1} of the proposed configuration
(c) i_{L2} of the proposed configuration

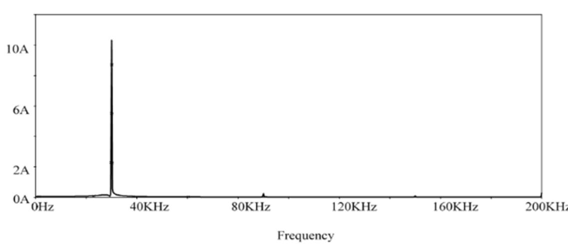

(a)

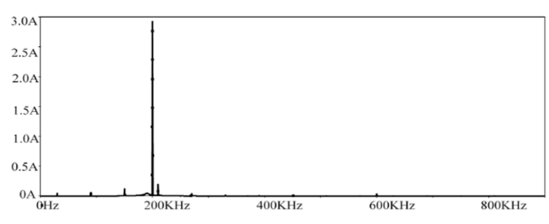

(b)

Fig. 6 Fourier analysis of currents with f_L= 30 kHz, f_H = 200 kHz
(a) i_{L1} of the proposed configuration
(b) i_{L2} of the proposed configuration

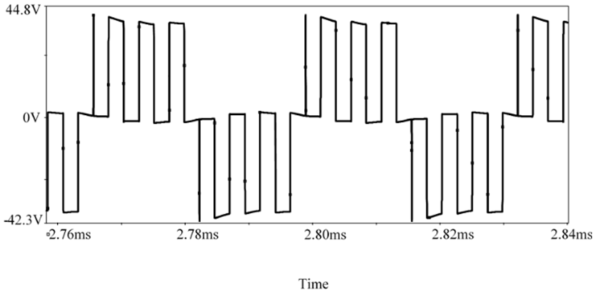

(a)

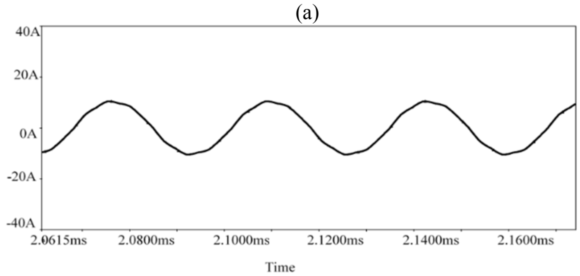

(b)

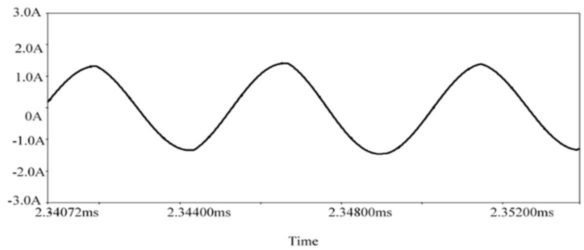

(c)
Fig. 7 Simulation waveforms with $f_L = 30$ kHz, $f_H = 210$ kHz
(a) v_{AB} of the proposed configuration
(b) i_{L1} of the proposed configuration
(c) i_{L2} of the proposed configuration

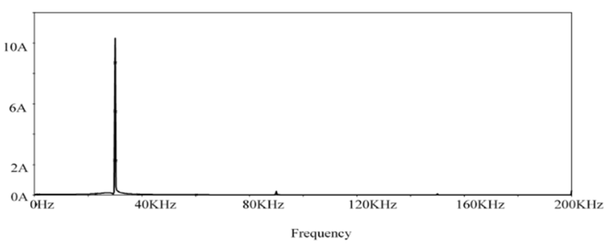

(a)

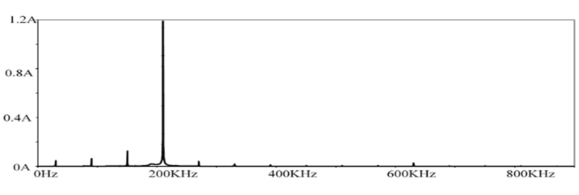

(b)
Fig. 8 Fourier analysis of currents with f_L= 30kHz, f_H = 210kHz
(a) i_{L1} of the proposed configuration
(b) i_{L2} of the proposed configuration

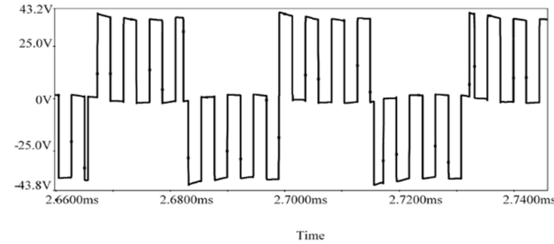

(a)

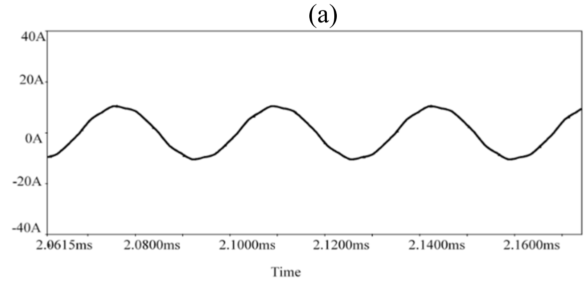

(b)

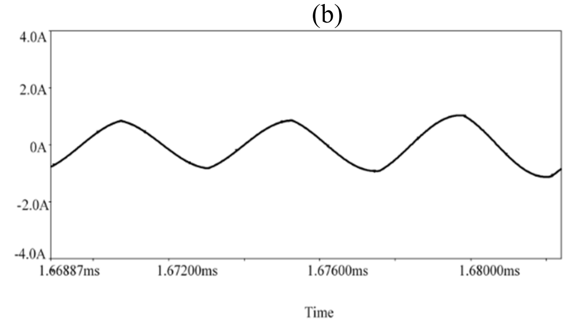

(c)
Fig. 9 Simulation waveforms with $f_L = 30$ kHz, $f_H = 220$ kHz
(a) v_{AB} of the proposed configuration
(b) i_{L1} of the proposed configuration
(c) i_{L2} of the proposed configuration

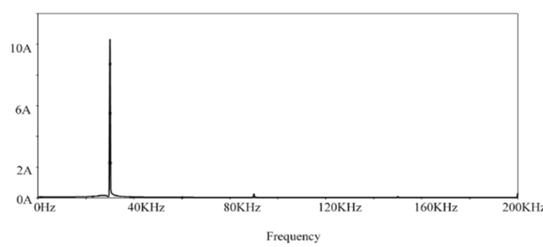

(a)

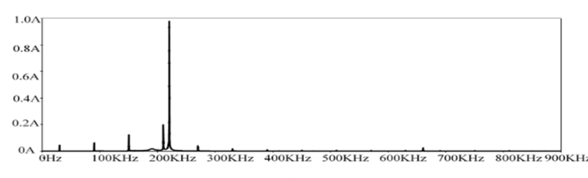

(b)
Fig. 10 Fourier analysis of currents with f_L= 30 kHz, f_H = 220 kHz
(a) i_{L1} of the proposed configuration
(b) i_{L2} of the proposed configuration

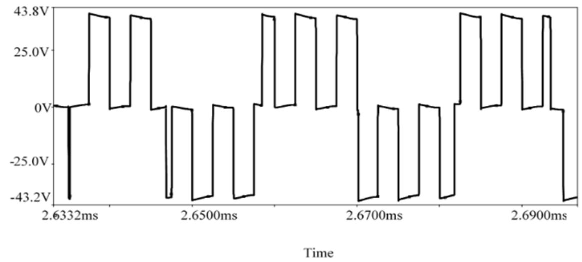

(a)

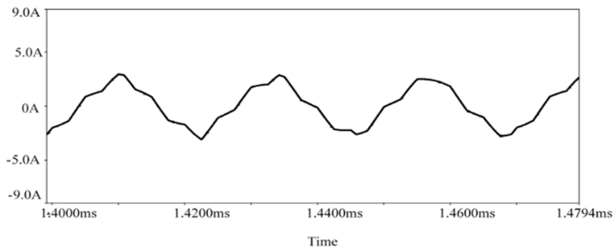

(b)

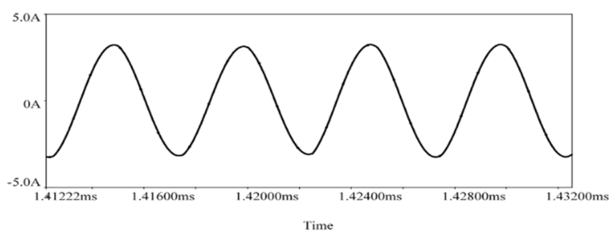

(c)

Fig. 11 Simulation waveforms with $f_L = 42.9$ kHz, $f_H = 200$ kHz
(a) v_{AB} of the proposed configuration
(b) i_{L1} of the proposed configuration
(c) i_{L2} of the proposed configuration

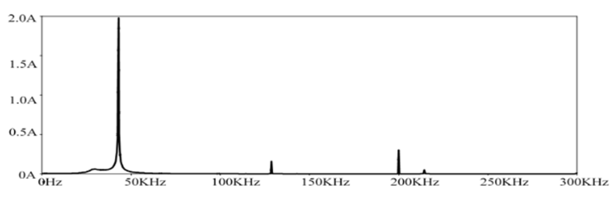

(a)

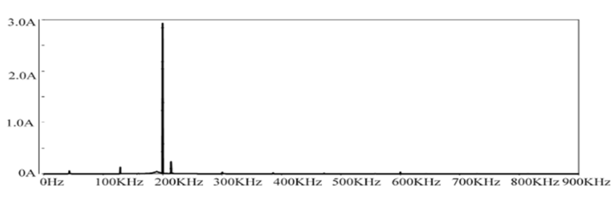

(b)

Fig. 12 Fourier analysis of currents with $f_L = 42.9$ kHz, $f_H = 200$ kHz
(a) i_{L1} of the proposed configuration
(b) i_{L2} of the proposed configuration

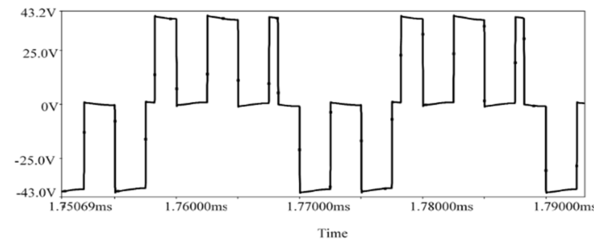

(a)

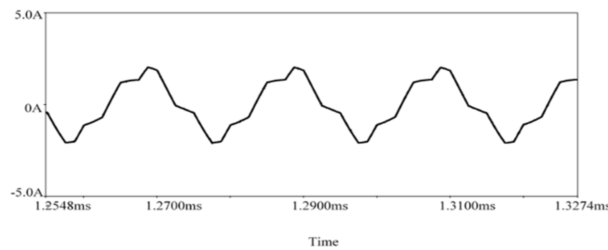

(b)

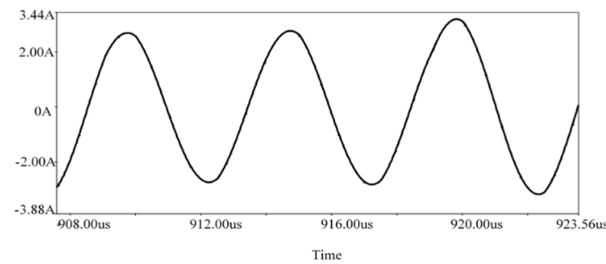

(c)

Fig. 13 Simulation waveforms with $f_L = 50$ kHz, $f_H = 200$ kHz
(a) v_{AB} of the proposed configuration
(b) i_{L1} of the proposed configuration
(c) i_{L2} of the proposed configuration

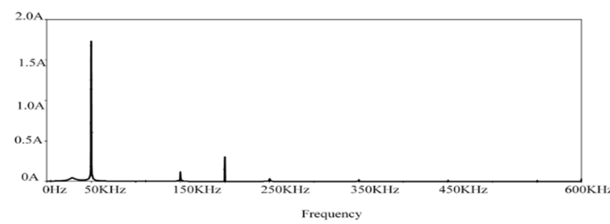

(a)

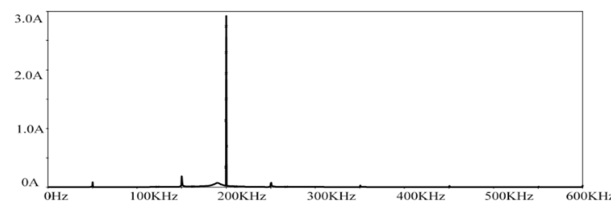

(b)

Fig. 14 Fourier analysis of currents with $f_L = 50$ kHz, $f_H = 200$ kHz
(a) i_{L1} of the proposed configuration
(b) i_{L2} of the proposed configuration

Fig. 11-14 display the independent control of load-1 by varying leg-1 lower switching frequency keeping leg-2 higher switching frequency fixed. Fig. 11 shows v_{AB}, i_{L1} and i_{L2} waveforms at f_{s1} = 42.9 kHz and f_{s2} = 200 kHz. Fig. 12 shows corresponding load current Fourier analysis at the above switching frequencies. Similarly, Fig. 13 shows v_{AB}, i_{L1} and i_{L2} waveforms at f_{s1} = 50 kHz and f_{s2} = 200 kHz and Fig. 14 shows corresponding load current Fourier analysis at the above switching frequencies.

Fig. 15 shows the variation of load-1 current with leg-1 lower switching frequency variation. We can observe that during this frequency variation load-2 current is constant. Similarly Fig. 16 shows the variation of load-2 current with leg-2 higher switching frequency variation. Here also we can observe that the load-1 current is constant. The above analysis shows the independent control of both loads with variable switching frequency control.

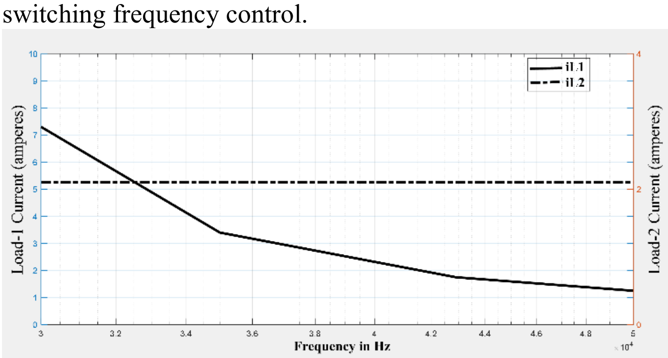

Fig. 15 Low frequency variation vs. currents in L_1 and L_2

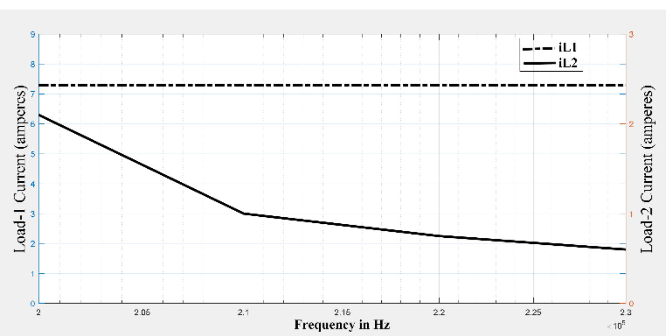

Fig. 16 High frequency variation vs. currents in L_1 and L_2

VI. Conclusion

Variable frequency controlled two-load IH cooking inverter is presented. Each load operates at different frequency. It also provides independent control of each load. Simulation results validate the performance of the presented system. The proposed configuration has the advantages like independent control, reduced component count, high efficiency and less complexity.

References

[1] N. A. Ahmed, M. Nakaoka, "Boost-half-bridge edge resonant soft switching PWM high-frequency inverter for consumer induction heating appliances," IEE Electric Power Applications, vol. 153, no. 6, 2006, pp. 932–938.

[2] Masaki Miyamae, Takahiro Ito, Kouki Matsuse, Masayoshi Tsukahara, "Performance of a High Frequency Quasi-Resonant Inverter with Variable-Frequency Output for Induction Heating", IEEE 7th International Power Electronics and Motion Control Conference, Harbin, China, 2012.

[3] Atsushi Fujita, Hideki Sadakata, Izuo Hirota, Hideki Omori, Mutsuo Nakaoka, "Latest Developments of High-Frequency Series Load Resonant Inverter Type Built-In Cooktops for Induction Heated All Metallic Appliances," *IPEMC'* 2009, pp. 2537-2544.

[4] S.M.W. Ahmed, M.M. Eissa, M. Edress, T.S. Abdel-Hameed, , "Experimental investigation of full bridge Series Resonant Inverters for Induction-Heating Cooking Appliances", 4th IEEE Conference on Industrial Electronics and Applications, ICIEA 2009, pp. 3327 – 3332.

[5] H. Fujita, H. Akagi, K. Sano, K. Mita, R. H. Leonard, "Pulse Density Modulation Based Power Control of a 4kW 400kHz Voltage-Source Inverter for Induction Heating Applications," Power Conversion Conference, Yokohama, 1993, pp. 111-116.

[6] Hector Sarnago, Oscar Lucia, Arturo Mediano, J.M. Burdio, "Class D/DE Dual-Mode-Operation Resonant Converter for Improved-Efficiency Domestic Induction Heating System," IEEE Transactions on Power Electronics, vol. 28, no. 3, March 2013, pp. 1274-1285.

[7] J. M. Burdio, L. A. Barragan, F. Monterde, D. Navarro, J. Acero, "Asymmetrical voltage-cancellation control for full-bridge series resonant inverters," IEEE Transactions on Power Electronics, vol. 19, no. 2, 2004, pp. 461 - 469.

[8] Jinfei Shen, Hongbin Ma,Wenxu Yan, Jing Hui, Lei Wu, "PDM and PSM Hybrid Power Control of a Series-Resonant Inverter for Induction Heating Applications", IEEE Conference on Industrial Electronics and Applications, ICIEA 2006.

[9] Jose M. Burdio, Fernando Monterde, Jose R. Garcia, Luis A. Barragan, Abelardo Martinez, "A Two-Output Series-Resonant Inverter for Induction-Heating Cooking Appliances," IEEE Transactions on Power Electronics, vol. 20, no. 4, 2005, pp. 815 - 822.

[10] F. Forest, E. Laboure, F. Costa, J.Y. Gaspard, "Principle of a multi-load / single converter system for low power induction heating," IEEE Trans. Power Electronics, vol.15, no. 2, 2000, pp. 223 - 230.

[11] Porpandiselvi, S., Vishwanathan, N.: 'Three-leg inverter configuration for simultaneous dual-frequency induction hardening with independent control', IET Power Electron. J., 2015, 8, (9), pp. 1571–1582.

[12] Lucıa, O., Maussion, P., Dede, E.: 'Induction heating technology and its applications: past developments, current technology, and future challenges', IEEE Trans. Ind. Electron., 2014, 61, (5), pp. 2509–2520.

[13] Porpandiselvi, S., Vishwanathan, N.: 'Single inverter configuration for simultaneous dual frequency induction hardening with independent control', Eur. Power Electron. Drives J., 2014, 24, (1), pp. 5–13